

Development and Validation of a New In-Situ Technique to Measure Total Gaseous Chlorine in Air

Teles C. Furlani¹, RenXi Ye¹, Jordan Stewart^{1,2}, Leigh R. Crilley¹, Peter M. Edwards², Tara F. Kahan³, Cora J. Young^{1*}

¹ Department of Chemistry, York University, Toronto, Canada

² Department of Chemistry, University of York, York, UK

³ Department of Chemistry, University of Saskatchewan, Saskatoon, Canada

*Correspondence to: youngcj@yorku.ca

Abstract

Total gaseous chlorine (TCl_g) measurements can improve our understanding of unknown sources of Cl to the atmosphere. Existing techniques for measuring TCl_g have been limited to offline analysis of extracted filters and do not provide suitable temporal information on fast atmospheric process. We describe high time-resolution in-situ measurements of TCl_g by thermolyzing air over a heated platinum (Pt) substrate coupled to a cavity ring-down spectrometer (CRDS). The method relies on the complete decomposition of TCl_g to release Cl atoms that react to form HCl, for which detection by CRDS has previously been shown to be fast and reliable. The method was validated using custom organochlorine permeation devices (PDs) that generated gas-phase dichloromethane (DCM), 1-chlorobutane (CB), and 1,3-dichloropropene (DCP). The optimal conversion temperature and residence time through the high-temperature furnace was 825 °C and 1.5 seconds, respectively. Complete conversion was observed for six organochlorine compounds, including alkyl, allyl, and aryl C-Cl bonds, which are amongst the strongest Cl-containing bonds. The quantitative conversion of these strong C-Cl bonds suggests complete conversion of similar or

26 weaker bonds that characterize all other TCl_g. We applied this technique to both outdoor and indoor
27 environments and found reasonable agreements in ambient background mixing ratios with the sum
28 of expected HCl from known long-lived Cl species. We measured the converted TCl_g in an indoor
29 environment during cleaning activities and observed varying levels of TCl_g comparable to previous
30 studies. The method validated here is capable of measuring in-situ TCl_g and has a broad range of
31 potential applications.

32 **1. Introduction**

33 Chlorine (Cl) containing compounds in the atmosphere can impact air quality, climate, and
34 health (Saiz-Lopez and Von Glasow, 2012; Simpson et al., 2015; Massin et al., 1998; White and
35 Martin, 2010). Gaseous chlorinated compounds are either organic (e.g., dichloromethane,
36 chloroform, and carbon tetrachloride) or inorganic (e.g., Cl₂, HCl, and ClNO₂), with inorganic Cl
37 being more reactive under most atmospheric conditions. In this work, total gaseous Cl (TCl_g) refers
38 to all gas-phase Cl-containing species weighted to their Cl content, including both inorganic and
39 organic species. While groups of chlorinated species are often considered based on reactivity
40 considerations (e.g., reactive chlorine, Cl_y), TCl_g includes all molecules that contain one or more
41 Cl atoms:

$$42 \text{ TCl}_g = 4*[\text{CCl}_4] + 3*[\text{CHCl}_3] + 2*[\text{CH}_2\text{Cl}_2] + [\text{CH}_3\text{Cl}] + 2*[\text{Cl}_2] + [\text{HOCl}] + \dots \quad \text{E1}$$

43 Impacts on air quality and climate are due to the high reactivity of atomic Cl produced by common
44 atmospheric reactions (e.g., photolysis and oxidation) of Cl-containing compounds (Haskins et al.,
45 2018; Riedel et al., 2014; Sherwen et al., 2016). The Cl cycle is important to atmospheric
46 composition in the stratosphere and troposphere, affecting species including methane, ozone, and
47 particles (both formation and composition), which influence air quality and climate (Solomon,
48 1999; Riedel et al., 2014; Young et al., 2014; Sherwen et al., 2016). High levels of some TCl_g

49 species (e.g., Cl₂ and carbon tetrachloride) are known to be toxic (White and Martin, 2010; Unsal
50 et al., 2021). The implications of many TCl_g species on human health are not well understood for
51 low level exposure for extended periods of time. Potential health impacts of organic chlorinated
52 compounds include hepatotoxicity, nephrotoxicity, and genotoxicity (Unsal et al., 2021;
53 Henschler, 1994). Impacts of inorganic chlorinated species include the chlorination of squalene, a
54 major part of human skin oils, by HOCl (Schwartz-Narbonne et al., 2019); respiratory irritation
55 and airway obstruction by Cl₂ (White and Martin, 2010); and increased incidence of asthma and
56 other chronic respiratory issues following exposure to chloramines (Massin et al., 1998).

57 Sources of Cl to the atmosphere are highly variable and depend on both direct emissions
58 and indirect regional Cl activation chemistry (Finlayson-Pitts, 1993; Raff et al., 2009; Khalil et al.,
59 1999). Direct emissions of TCl_g can come from numerous natural and anthropogenic activities
60 such as, but not limited to, ocean and volcanic emissions, biomass burning, disinfection (i.e.,
61 household cleaning, pool emission, etc), use of solvents and heat transfer coolants, and incineration
62 of chlorinated wastes (Blankenship et al., 1994; Lobert et al., 1999; Keene et al., 1999; Butz et al.,
63 2017; Wong et al., 2017; Fernando et al., 2014). Activation of Cl is another source, occurring when
64 atmospheric processes transform relatively unreactive chloride (Cl⁻, such as sea salt, NaCl) into
65 reactive gaseous chlorine (Cl_y), which will contribute to TCl_g. Understanding global levels of TCl_g
66 is difficult due to complex emissions and chemistry. Our best estimates come from modelling
67 studies combined with collaborative efforts to compose policy reports on halogenated substances,
68 such as the World Meteorological Organization (WMO) Scientific Assessment of Stratospheric
69 Ozone Depletion (WMO (World Meteorological Organization), 2018). Mixing ratio estimates of
70 halogenated species from this report are summed from individual measurements (e.g., National
71 Oceanic and Atmospheric Administration (NOAA) and Advanced Global Atmospheric Gases

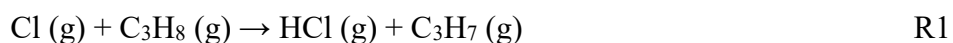
72 Experiment (AGAGE)). The WMO report includes flask (captured gas from clean air sectors) and
73 in-situ measurements from field campaigns and routine sampling sites (e.g., CONvective
74 Transport of Active Species in the Tropics (CONTRAST)) (Prinn et al., 2018; Pan et al., 2017;
75 Andrews et al., 2016; Montzka et al., 2021; Adcock et al., 2018). In the most recent WMO report
76 (2018), a decrease of 12.7 ± 0.9 pptv Cl yr⁻¹ in total tropospheric Cl was determined for Montreal
77 Protocol-controlled substances (e.g., chlorofluorocarbons (CFCs) and hydrochlorofluorocarbons
78 (HCFCs)). The decrease in Montreal Protocol-controlled emissions has been slightly offset by an
79 increase in relatively short-lived substances (e.g., dichloromethane) that are not controlled by the
80 Montreal Protocol (WMO (World Meteorological Organization), 2018). Despite the emissions of
81 these regulated chlorinated species being relatively well-constrained, new sources for some of
82 these compounds have appeared in the recent past. For example, unexpected increases observed in
83 CFC-11 emissions suggested new unreported production (WMO (World Meteorological
84 Organization), 2018). A new source of chloroform was also recently identified and attributed to
85 halide containing organic matter derived from penguin excrement in the Antarctic tundra (Zhang
86 et al., 2021). Atmospheric levels of TCl_g will additionally be impacted by emission sources that
87 are relatively poorly constrained, including combustion and disinfection. Increasing levels of
88 chlorinated species from known and unknown pathways was observed in a recent ice core study,
89 which estimated an increase of up to 170% of Cl_y (= BrCl + HCl + Cl + ClO + HOCl + ClNO₃ +
90 ClNO₂ + ClOO + OClO + 2·Cl₂ + 2·Cl₂O₂ + ICl) from preindustrial times to the 1970s could be
91 attributed to mostly anthropogenic sources (Zhai et al., 2021).

92 Understanding TCl_g source and sink chemistry is not only important for the ambient
93 atmosphere but also for indoor environments. Uncertainty in sources and levels of chemicals,
94 including Cl-containing compounds, indoors is related to heterogeneity in sources and individual

95 indoor environments, and the fact that relatively few studies have focused on indoor chemistry
96 compared to outdoor. The role of chlorinated species on indoor air quality has been investigated
97 in a few studies (Mattila et al., 2020; Wong et al., 2017; Dawe et al., 2019; Giardino and Andelman,
98 1996; Shepherd et al., 1996; Doucette et al., 2018; Nuckols et al., 2005). Most studies have focused
99 on cleaning with Cl-based cleaners, in which HOCl and other inorganic compounds have been
100 observed in the gas phase at high levels (Wong et al., 2017; Wang et al., 2019; Mattila et al., 2020).
101 Some studies have reported the presence of organic chlorinated species such as chloroform and
102 carbon tetrachloride above bleach cleaning solutions indoors (Odabasi, 2008; Odabasi et al., 2014),
103 and chloroform has been observed during water-based cleaning activities, such as showering and
104 clothing washing (Nuckols et al., 2005; Shepherd et al., 1996; Giardino and Andelman, 1996).

105 Constraining the Cl budget is critical to better understanding its contributions to climate,
106 air quality, and human health. Robust total Cl measurements are useful because it is not always
107 feasible to routinely deploy individual measurements of the large number of known Cl-containing
108 compounds (Table S1). As described above, estimates of TCl_g from models and summed
109 measurements have demonstrated gaps in our knowledge. It is therefore essential to have a method
110 capable of measuring true TCl_g to explain discrepancies between model and measured estimates
111 due to unknown species. Measurements of total elemental composition in the condensed phase,
112 including total Cl, have been used for monitoring and managing both known and unknown
113 compounds (Miyake et al., 2007c, a; Yeung et al., 2008; Miyake et al., 2007b; Kannan et al., 1999;
114 Xu et al., 2003; Kawano et al., 2007). However, TCl_g methods have been limited to offline analysis
115 of scrubbed sample gas (e.g., flue); these methods rely on multiple extraction steps and the
116 application of condensed-phase total Cl analyses, such as combustion ion chromatography
117 (Miyake et al., 2007a; Kato et al., 2000) or neutron activation analysis (Berg et al., 1980; Xu et al.,

118 2006, 2007). Because offline techniques suffer from extraction uncertainties and do not have the
119 temporal resolution to effectively probe fast chemistry in the atmosphere, in-situ measurements of
120 total elemental gaseous composition have been developed for several elements (Hardy and Knarr,
121 1982; Veres et al., 2010; Roberts et al., 1998; Maris et al., 2003; Yang and Fleming, 2019). For
122 example, total nitrogen has been measured using Pt-catalyzed thermolysis coupled to online
123 chemiluminescence detection (Stockwell et al., 2018). Using a similar approach, we describe here
124 a method for TCl_g , where catalyzed thermolysis is coupled to a high time-resolution HCl cavity
125 ring-down spectrometer (CRDS). This technique relies on the complete thermolysis of TCl_g , which
126 yields chlorine atoms. These Cl atoms readily form HCl via hydrogen abstraction (R1), in this case
127 from propane (or its thermolysis products) that is supplied in excess.



128 The objectives of this paper are to: (i) Develop and validate an instrument capable of in-
129 situ measurement of TCl_g through conversion to HCl and detection by CRDS; and (ii) demonstrate
130 application of the technique to outdoor and indoor TCl_g measurements.

131 **2. Materials and experimental methods**

132 **2.1. Chemicals**

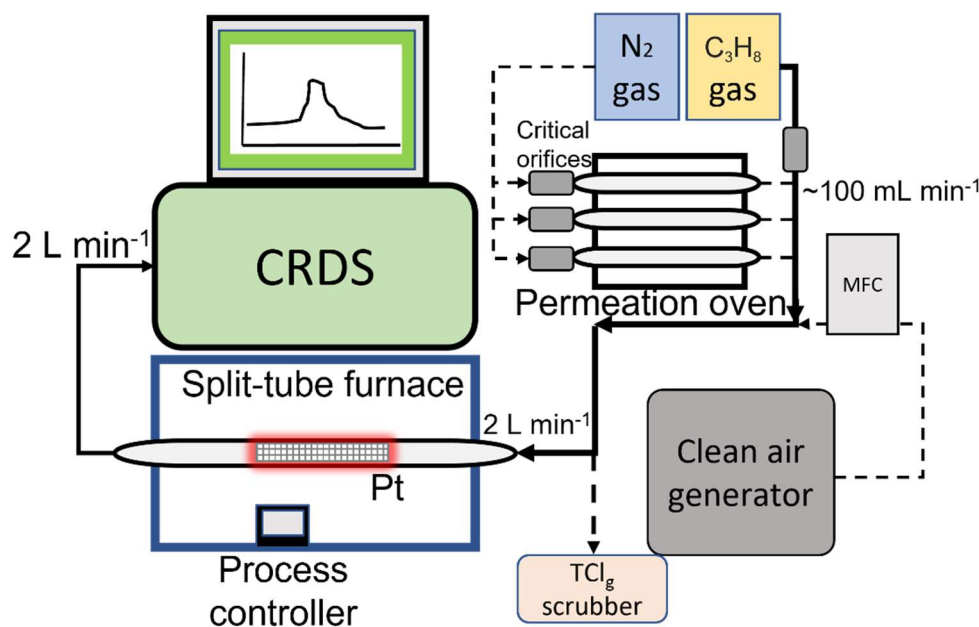
133 Commercially available reagents were purchased from Sigma-Aldrich (Oakville, Ontario,
134 Canada): dichloromethane (DCM, HPLC grade), 1-chlorobutane (CB, 99.5%), cis-1,3-
135 dichloropropene (DCP, 97%), trichlorobenzene (TrCB, 99%), tetrachlorobenzene (TeCB, 98%),
136 pentachlorobenzene (PeCB, 96 %), sodium chloride, and 52 mesh sized platinum catalyst (99.9
137 %). Toluene (HPLC grade) was purchased from BDH VWR (Mississauga, Ontario, Canada).
138 Nitrogen (grade 4.8) and propane (C_3H_8 , 12.7% in nitrogen, v/v) gas was from Praxair (Toronto,
139 Ontario, Canada). Experiments used deionized water generated by a Barnstead Infinity Ultrapure
140 Water System (Thermo Fisher Scientific, Waltham, Massachusetts, USA; $18.2 \text{ M}\Omega \text{ cm}^{-1}$). A

141 permeation device (PD) described previously was used to generate gaseous HCl (Furlani et al.,
142 2021). Chlorine-free zero air was generated by a custom-made zero-air generator.

143 **2.2. HCl and total chlorine (HCl-TCI) instrument**

144 The main components of the HCl-TCI (Figure 1) are platinum catalyst mesh, a quartz glass
145 flow tube, a split-tube furnace (Protégé Compact, 1100°C max temperature, Thermcraft
146 incorporated, North Carolina, USA), and a CRDS HCl analyzer (Picarro G2108 Hydrogen
147 Chloride Gas Analyzer). The platinum catalyst consisted of ~2 g platinum mesh with a total
148 combined surface area of 134 cm². Sample gas was mixed with critical orifice-regulated (Lenox
149 laser, Glen Arm, Maryland, USA, 30 psi; SS-4-VCR-2-50) propane gas (62 ± 6 standard cubic
150 centimetres per minute (sccm)), provided in excess prior to introduction to the furnace to promote
151 (R1). The added propane does not fully thermolyze at temperatures < 650 °C, which can lead to
152 spectral interferences in the CRDS analyzer (Figure S1) and should only be added when
153 temperatures exceed 650°C (Furlani et al., 2021). All lines and fittings were made of
154 perfluoroalkoxy (PFA) unless stated otherwise. The mixing line carrying clean air dilution flows
155 was controlled by a 10 L min⁻¹ mass flow controller (MFC, GM50A, MKS instruments, Andover,
156 Massachusetts, USA). The length of the sample gas tubing to the furnace was 0.6 m, and the
157 transfer line between the furnace and CRDS was 0.2 m. The furnace transfer line met an overflow
158 tee when delivering flows greater than the CRDS flowrate of 2 L min⁻¹. The coupled CRDS can
159 capture transient fast HCl formation processes on the timescale of a few minutes, limited by the
160 high adsorption activity of HCl on inlet surfaces (discussed further in Section 3.3). The CRDS
161 collects data at 0.5 Hz. Limits of detection (LODs) for the CRDS were calculated as three times
162 the Allan–Werle deviation in raw signal intensity when overflowing the inlet with zero air directed

163 into the CRDS for ~ 10 h. The 30-sec LOD is 18 pptv and well below expected HCl from TCI_g
164 conversion (Furlani et al., 2021).



165
166 **Figure 1.** Sampling schematic showing the key components of the HCl-TCI coupled to the CRDS
167 analyzer. Dashed lines indicate parts of the apparatus used only during validation. Not to scale.

168 2.3. Preparation of organochlorine permeation devices (PDs)

169 Organochlorine PDs were prepared as follows: approximately 200 μL of DCM, CB, or DCP
170 was pipetted into a 50 mm PFA tube (3 mm i.d. with 1 mm thickness), thermally sealed at one end
171 and plugged at the other end with porous polytetrafluoroethylene (PTFE) (13 mm length by 3.17
172 mm o.d.). The polymers allow a consistent mass of standard gas to permeate at a given temperature
173 and pressure. The method for temperature and flow control of the PDs is described in detail in Lao
174 et al. (2020). Briefly, an aluminum block that was temperature-controlled (OmegaTM; CN 7823,
175 Saint-Eustache, QC, Canada) using a cartridge heater (OmegaTM; CIR-2081/120V, Saint-Eustache,
176 QC, Canada) housed the PD and was regulated to 30.0 ± 0.1 °C. Dry N₂ gas flowed through a PFA
177 housing tube (1.27 cm o.d.) in the block that contained the PD. Stable flows of carrier gases passed
178 through the housing tube in the oven were achieved using a 50 μm diameter critical orifice (Lenox

179 laser, Glen Arm, Maryland, USA, 30 psi; SS-4-VCR-2-50) and were 120 ± 12 , 99 ± 9.9 and 120
180 ± 12 sccm for DCM, CB, and DCP, respectively. Flows were measured using a DryCal Definer
181 220 (Mesa Labs, Lakewood, Colorado, USA). The mass emission rate of each organochlorine from
182 the PDs was quantified gravimetrically over a period of approximately 4 weeks (mass accuracy \pm
183 0.001 g). Mass emission rates for each PD were determined as 640 ± 10 , 240 ± 40 , and 1.20×10^4
184 $\pm 0.02 \times 10^4$ ng min⁻¹ (n=3, $\pm 1\sigma$) at 30 °C for DCM, CB, and DCP, respectively.

185 **2.4. HCl-TCl optimization**

186 Gas phase standards of DCM, CB, and DCP were used to test the conversion efficiency of
187 chlorinated compounds to form HCl. Bond dissociation energies for carbon-Cl bonds typically
188 range between 310 and 410 kJ mol⁻¹ (Tables S1, S2). The split-tube furnace has a process controller
189 capable of increasing or decreasing temperature at a set °C min⁻¹, which allowed us to identify the
190 temperature at which enough energy was provided to break the bonds. By introducing a consistent
191 amount of each of the organochlorines, separately, to the HCl-TCl set over a simple temperature
192 ramping program we could monitor in real-time the conditions necessary to break the bonds by
193 measuring the formation of the resulting HCl. The operating temperature was determined when
194 complete conversion of the measured TCl_g for the tested compounds was sustained at 100%
195 conversion based on PD emission rates.

196 To determine the optimal residence time in the quartz tube with the Pt catalyst, flows of
197 0.6–5.5 L min⁻¹ containing DCM sample gas in clean air were tested yielding a range of residence
198 times between 0.5 and 4.5 sec in the furnace. Temperature remained constant at 825 °C throughout
199 the experiment, and a dilution flow of 4.0 L min⁻¹ of clean air was added to the sample flow exiting
200 the furnace before introduction to the CRDS.

201 We tested the HCl transmission of the HCl-TCl at 2 mixing ratios (18 and 10 ppbv) using
202 a 12 M HCl PD with zero air dilution flows of 3.5 or 5 L min⁻¹ using a 5 L min⁻¹ MFC (GM50A,
203 MKS instruments, Andover, Massachusetts, USA). The HCl recovery through the furnace was
204 tested by comparing measured HCl mixing ratios through HCl-TCl to those with the furnace flow
205 tube replaced by a similar length of tubing. A heat gun (Master Varitemp® vt-750c) was used to
206 heat the flow tube entrance to ~80 °C to minimize HCl sorption. We tested the HCl-TCl conversion
207 efficiency for 5 different mixing ratios of three organochlorine PD standards (DCM, CB, and DCP)
208 under three conditions: (1) both Pt catalyst and added propane, (2) only Pt catalyst, and (3) only
209 added propane. Each gas was tested individually under the same conditions; sample gas from PDs
210 was mixed with propane and immediately diluted into clean air using a 10 L min⁻¹ MFC. The
211 dilution flows ranged from 2.2–9.0 L min⁻¹. The sampling lines were the same lengths as stated
212 previously. In this experiment, the CRDS flowrate of 2 L min⁻¹ was sufficient to give an optimal
213 residence time of 1.5 sec through the HCl-TCl (see Section 3.1). In all experiments the CRDS
214 subsampled through the furnace from the main transfer line and the excess gas was directed
215 outdoors through a waste line containing a carbon trap (Purakol, Purafil, Inc, Doraville, Georgia,
216 USA). We also tested the HCl-TCl conversion efficiency for two different quantities of three
217 chlorobenzenes (TrCB, TeCB, and PeCB). Due to their high boiling points, PDs of these
218 compounds could not be prepared. Instead, small volumes of approximately 1 mM solutions of
219 these compounds dissolved in toluene were directly introduced to the HCl-TCl while it was
220 sampling room air. Room air measurements of TCl_g were consistently >1 ppbv. These were
221 measured before each experiment and did not affect the peak integration described below. With a
222 short piece of tubing used as an inlet, 1 and 2 μL of each compound was injected onto the inner
223 surface of the tubing, which was heated to ~100 °C with a heat gun to facilitate volatilization. The

224 resulting signals were integrated over a time period of 2.5 hours to obtain the total quantity of HCl
225 detected by the CRDS, which was used to calculate conversion efficiency. To account for
226 uncertainties in peak integration, a high and low peak area boundary was determined, with the
227 average peak area taken for each injection. Duplicates of each injected quantity were performed,
228 except for 1 μL TrCB, which was performed in triplicate.

229 To determine if there was any positive bias in the TCl_g measurement from the conversion
230 of particulate chloride (pCl^-), NaCl aerosols were generated by flowing 2 L min^{-1} of chlorine free
231 zero air through a nebulizer containing a solution of 2% w/w NaCl in deionized water. The aerosol
232 flow was then mixed with 1 L min^{-1} of chlorine free dry zero air to achieve a total flow of 3 L
233 min^{-1} , The HCl-TCl (2 L min^{-1}) then sampled off this main mixing line. Chloride was added after
234 monitoring background zero air levels. After ~ 3 hours of measuring the converted pCl^- , a PTFE
235 filter ($2 \mu\text{m}$ pore size, 47 mm diameter, TISCH scientific, North Bend, Ohio, USA) was added
236 inline onto the inlet of the HCl-TCl.

237 **2.5. Outdoor air HCl-TCl measurements**

238 Outdoor air sampling was performed between 00:00 on July 7 to 20:00 on July 11, 2022
239 (Eastern daylight time, EDT). The sampling site was the air quality research station located on the
240 roof of the Petrie Science and Engineering building at York University in Toronto, Ontario,
241 Canada (43.7738° N , 79.5071° W , 220 m above sea level). The HCl-TCl was co-located with a
242 Campbell Scientific weather station paired with a cr300 datalogger. All inlet lines and fittings were
243 made of PFA unless stated otherwise. All indoor inlet lines and fittings were kept at room
244 temperature. A mass flow controller (GM50A, MKS instruments, Andover, Massachusetts, USA)
245 regulated a sampling flow of 14.7 L min^{-1} using a diaphragm pump through a 2.4 m sampling inlet
246 (I.D. of 0.375") from outdoors. The outdoor air was pulled through a $2.5 \mu\text{m}$ particulate matter

247 cut-off URG Teflon Coated Aluminum Cyclone (URG Corporation, Chapel Hill, North Carolina,
248 USA) to remove larger particles and then passed through a PTFE filter (2 μm pore size, 47 mm
249 diameter, TISCH scientific, North Bend, Ohio, USA). The CRDS subsampled 2 L min^{-1} through
250 the furnace off the main inlet line, yielding a total inlet flow of 16.7 L min^{-1} . The apparatus had
251 zero air overflow the inlet 1 hour prior to and after outdoor sampling. The CRDS sample flow
252 passed first through a PTFE filter (2 μm pore size, 47 mm diameter) and then two high efficiency
253 particulate air (HEPA) filters contained within the CRDS outer cavity metal compartment heat-
254 regulated to 45 $^{\circ}\text{C}$. Instances of flagged instrument errors in the CRDS data during ambient
255 observations were removed as standard practice in quality control procedures.

256 **2.6. Indoor air HCl-TCl and HOCl analyzer measurements**

257 To test indoor applications of the HCl-TCl, a 1 m^2 area of laboratory floor was cleaned with
258 a commercial spray bottle cleaner (1.84 % sodium hypochlorite w/w) and emissions were
259 compared with an HOCl analyzer. The HOCl analyzer is a commercial instrument designed to
260 quantify gaseous hydrogen peroxide (H_2O_2) using CRDS (Picarro PI2114 Hydrogen Peroxide
261 Analyzer; Picarro Inc.). The instrument is also sensitive to HOCl due to similar absorbance
262 wavelengths of their first overtone stretches in the near IR. The wavelengths monitored have been
263 altered to selectively detect HOCl. Details on instrument calibration and validation are provided
264 in Stubbs et al. (2022).

265 The distance from the suspended 2 m inlet lines of both instruments to the floor was ~ 1 m.
266 The flowrate through the furnace and inlet was the 2 L min^{-1} CRDS flowrate. The flowrate for the
267 HOCl analyzer was 1 L min^{-1} . The sectioned off area was cleaned four times, spraying 32 times
268 for each application using the commercial cleaner. Three of these events were measured using the
269 HCl-TCl and HOCl analyzer, while one event was measured using the HCl CRDS only.

270 **3. Results and Discussion**

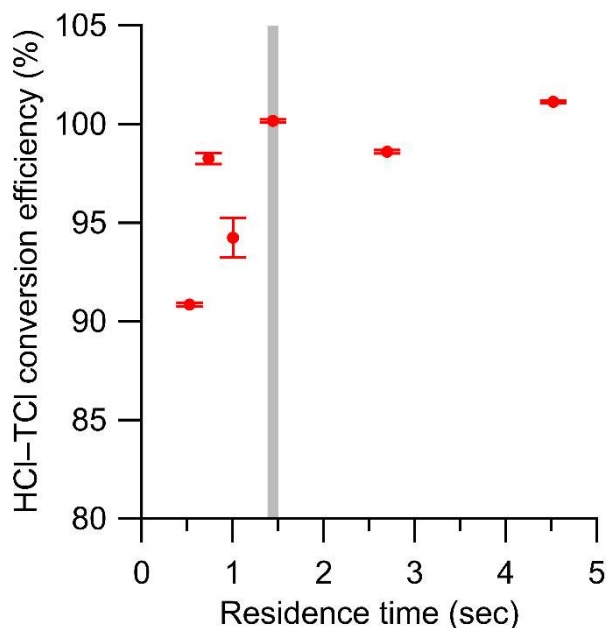
271 **3.1. HCl-TCl temperature and residence time optimization**

272 We validated this method by testing conversion efficiency of organochlorines under different
273 operating parameters and conditions. Testing all TCl_g species is not feasible, but by testing
274 compounds that contain strong Cl-containing bonds, we infer at least equal efficacy of the system
275 in the breakage of relatively weaker Cl-containing bonds (Tables S1 and S2). We selected strong
276 Cl-containing bonds (i.e., alkyl, allyl, and aryl chlorides) and used them as a proxy for compounds
277 containing weaker Cl bonds; therefore, by demonstrating their complete conversion we set
278 precedent for conversion of all TCl_g. The temperature of the furnace is a key factor in
279 accomplishing complete thermolysis, and the minimum temperature of the furnace containing the
280 Pt catalyst to break the C-Cl bonds in DCM was determined. A simple temperature ramping
281 program was used to determine the breakthrough temperature. The temperature was increased at a
282 rate of 2.7 °C min⁻¹ starting at 300 °C and ending at 800 °C. The temperature breakthrough was
283 observed when complete conversion of the expected HCl for the tested compounds (based on PD
284 emission rate) was stable after reaching the optimal temperature. It was found to be ~800 °C for
285 the tested organochlorines (Figure S2).

286 Determining the optimal residence time of sample gas in the HCl-TCl is also essential for
287 an optimized TCl_g conversion method. Using a temperature slightly above the observed
288 breakthrough temperature of 800 °C determined above (825 °C), six residence times were tested
289 with DCM, ranging from 0.5 to 4.5 seconds in the HCl-TCl (Figure 2). At each residence time the
290 conversion efficiency was determined, where conversion efficiency was calculated as follows:

$$291 \text{ Conversion efficiency} = \frac{\text{Measured TCl}_g}{\text{Expected TCl}_g} \times 100 \% \quad \text{E2}$$

292 The optimal residence time was ~ 1.5 seconds, corresponding to a conversion efficiency of 100.1
293 ± 0.1 %. The uncertainty in conversion efficiency measurements is the variability in the measured
294 HCl signal for 30 minutes after a signal plateau was observed. The reported uncertainty does not
295 include uncertainties in mixing, or turbulence induced surface effects, which we cannot quantify.
296 When residence times were lower (i.e., sample gas traveled more quickly through the system) than
297 1.5 seconds, the conversion efficiencies were lower by 2 – 10 %, the measured HCl signal was
298 more erratic, and it took longer to stabilize. When residence times were higher (i.e., sample gas
299 traveled more slowly through the system) than 1.5 seconds, the conversion efficiencies were
300 comparable (± 2 %), but the measured HCl suffered from longer equilibration times (~ 30 minutes,
301 more than double the 1.5 residence time) and therefore a slower response time, likely due to
302 increased surface effects of HCl after exiting the furnace. An optimal residence time of 1.5 seconds
303 was selected for all HCl-TCl experiments for its good conversion efficiency and reasonable
304 response time (see Table S3).



305
306 **Figure 2.** Conversion efficiency of DCM plotted against residence time in the HCl-TCl at 825 °C.
307 Error bars represent the percent relative standard deviation of the measured HCl by the CRDS over

308 ~30 minutes, after signal has plateaued. Grey vertical line denotes the selected residence time.
309 Note that the error bars are represented by the precision of the instrument, and we expect there
310 would be greater experiment-to-experiment variability.

311

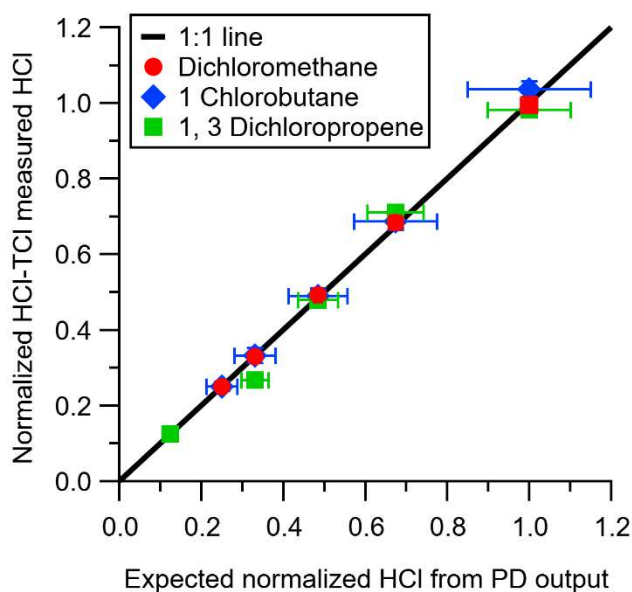
312 **3.2. HCl-TCl conversion efficiency**

313 The efficiency of HCl throughput in the HCl-TCl was tested. Initial tests resulted in
314 transmission efficiencies of $81.2\% \pm 1.4$ ($n = 3$) and 88.1% ($n = 1$) for 18 ppbv and 10 ppbv HCl,
315 respectively. At the inlet to the furnace, a small piece of the quartz tube is not heated. We
316 hypothesized that complete transmission of HCl was hindered through sorption to that portion of
317 quartz tube. Repeating the experiment with heat applied led to increased throughput efficiencies
318 of 85.7% (18 ppbv, $n = 1$) and 93.9% (10 ppbv, $n = 1$). Therefore, good HCl throughput efficiency
319 was demonstrated overall, with the cause of minor HCl losses identified to be sorption losses to
320 room temperature glass. Conversion of particulate chloride (pCl^-) was observed to take place in
321 the HCl-TCl (Figure S3), but once a filter was introduced the signal returned to background levels.
322 Thus, to capture only gaseous TCl_g from samples that may contain particulate chloride, a
323 particulate filter should be used.

324 The conversion efficiency of each of the two alkyl chlorine and one allyl chlorine compounds
325 using the HCl-TCl was tested at 5 different mixing ratios. See Table S4 for summary of mixing
326 ratios used; all lower mixing ratios were generated by diluting the highest mixing ratio of each
327 compound by chlorine-free zero air. All three showed good linearity and near 1:1 correlation with
328 the HCl expected to be formed from the PD under standard operating conditions (Figure 3). Due
329 to differences in PD emission rates, the values in Figure 3 are normalized to the highest mixing
330 ratio to visualize comparisons more easily. With both Pt and propane the HCl-TCl conversion was
331 99.6 ± 3.2 , 104.8 ± 5.6 , and $102.7 \pm 7.8\%$ for DCM, CB, and DCP, respectively (Table 1), as the
332 average conversion efficiency \pm relative standard deviation. From Figure 3 the comparison

333 between expected and measured TCl_g is illustrated by near unity in the orthogonal distance
334 regression slope ($\pm 1\sigma$, the error in the regression analysis), and was 0.996 ± 0.012 , 1.048 ± 0.060 ,
335 and 1.027 ± 0.061 for DCM, CB, and DCP, respectively. With only the Pt catalyst, the HCl-TCl
336 conversion was 80.7 ± 0.4 , 54.1 ± 1.6 , and $54.3 \pm 3.5\%$ for DCM, CB, and DCP, respectively
337 (Figure S4, Table 1). This result indicates the added hydrogen source (propane) is needed to
338 promote R1. Although necessary in this laboratory scenario, some ambient conditions may be rich
339 enough in hydrogen-containing molecules that excess propane is not needed. However, providing
340 propane in excess ensures the presence of an abundance of hydrogen atoms that can be readily
341 abstracted by Cl atoms via R1. When the Pt catalyst was removed, the HCl-TCl conversion was
342 94.4 ± 4.6 , 44.2 ± 0.9 , and $41.7 \pm 3.4\%$ for DCM, CB, and DCP, respectively (Figure S4, Table
343 1). The observed dependence of the Pt catalyst indicates that a reactive surface is important

344



345

346 **Figure 3.** HCl measured by CRDS plotted against the expected HCl from HCl-TCl converted
347 DCM (red circle), 1-chlorobutane (blue diamond), and 1,3-dichloropropene (green square) under
348 condition (1). All values are normalized to the highest expected HCl concentration to better
349 illustrate deviations from unity (black line). Error bars on the y-axis represent 1σ in the HCl signal

350 over 10 minutes. Error bars on the x-axis represent the uncertainty in the PD used to generate
351 DCM.

352 **Table 1.** Conversion efficiency for tested Cl-containing compounds under different conditions
353 (both Pt and propane; Pt only; propane only). Note that chlorobenzenes were only tested under
354 final Pt and propane conditions.

Tested TCl _g species	Cl bond dissociation energy (kJ mol ⁻¹)	Conversion efficiency (%)		
		Pt and propane	Pt only	Propane only
Dichloromethane (DCM) ^a	310	99.6 ± 3.2	80.7 ± 2.4	94.4 ± 6.6
1-Chlorobutane (CB) ^a	410	104.8 ± 5.6	54.1 ± 6.6	44.2 ± 5.9
1, 3-Dichloropropene (DCP) ^a	350	102.7 ± 7.8	54.3 ± 5.2	41.7 ± 5.1
Trichlorobenzene (TrCB) ^b	400	97.0 ± 19.9		
Tetrachlorobenzene (TeCB) ^b	400	90.6 ± 10.3		
Pentachlorobenzene (PeCB) ^b	400	90.2 ± 14.8		

355 ^aConversion efficiency was determined from the orthogonal distance regression slope and ± σ and propagated error
356 from individual permeation devices.

357 ^bConversion efficiency was determined directly by the quantity (mol) of HCl measured from liquid injections of 1
358 mM standards. The error represents ±σ of measurements for n = 5 (TrCB) or n = 4 (TeCB, PeCB) injections.

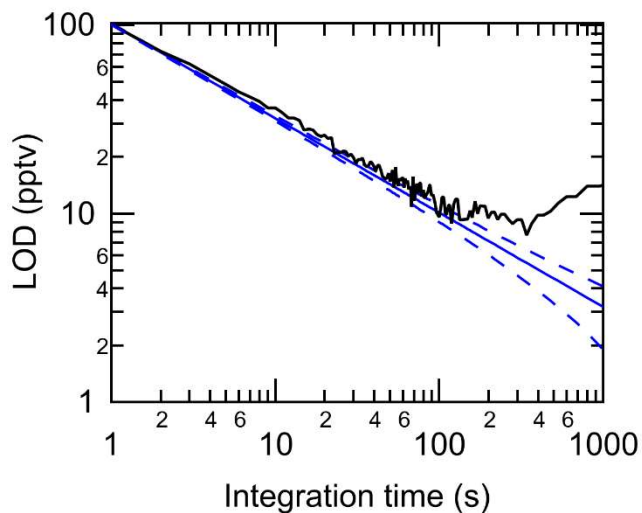
359
360 to achieve complete thermolysis at 825 °C. The relatively higher conversion for DCM in the
361 absence of the Pt catalyst or hydrogen source may be attributed to its lower bond dissociation
362 energy (310 kJ mol⁻¹) compared to estimated bond dissociation energies for CB and DCP (CB
363 inferred from Table S2 (~410 kJ mol⁻¹), and DCP from tetrachloroethylene (350 kJ mol⁻¹ in Table
364 S1)). It is possible that a higher temperature could lead to full conversion of TCl_g in the absence
365 of Pt catalyst; however, that was not explored in this study. To further validate the HCl-TCl, the
366 conversion efficiency of three aryl chlorine compounds were tested under the final operating
367 conditions (i.e., in the presence of both Pt and added propane). The TCl_g measured from the three
368 aryl compounds was unity, within the uncertainty of the measurement (Table 1).

369 The results for all six compounds show that the HCl-TCl is capable of complete conversion
370 of mono and polychlorinated species on sp³ and sp² carbons using the determined temperature and
371 flow conditions. The complete thermolysis of the strongest C-Cl bond on the primary alkyl
372 chloride (CB) demonstrates the efficacy of the HCl-TCl. Breaking these relatively strong C-Cl

373 bonds, with consistent conversion efficiency across alkyl, allyl, and aryl C-Cl bonds, is a good
374 proof of concept for complete conversion of all bonds of similar or weaker bond energies that
375 characterize all other TCl_g. To practically validate the HCl-TCl under real-world conditions with
376 atmospherically relevant TCl_g mixtures and mixing ratios we also deployed and configured the
377 system to measure outdoor and indoor air.

378 **3.3. Performance metrics of HCl-TCl**

379 Using a flow of zero air through the HCl-TCl, method limits of detection (LODs) were
380 calculated as three times the Allan-Werle deviation (Figure 4) when overflowing a 20 cm inlet
381 (3.17 mm i.d.) with zero air for one hour. The LODs determined in the measurements for 2 second,
382 1 minute, 5 minute, and 1 hour integration times were 73, 15, 10, and 8 pptv, respectively. The
383 response time of the instrument was assessed during experiments with DCM, CB, and CP. The
384 time for the signal to decay after removal of the PDs was determined to 37 % (1/e) and 90 % (t₉₀)
385 of the maximum signal. The maximum time to achieve 1/e was 23 seconds, while the maximum
386 time to achieve t₉₀ was 189 seconds (Table S3). These are comparable to the response times for
387 the HCl CRDS instrument itself (Furlani et al. 2021), suggesting the addition of the inlet furnace
388 has a modest impact on the residence time. Given the high mixing ratios used to test the response
389 times, we argue that under most conditions relevant to indoor and outdoor atmospheric chemistry,
390 a sample integration time of one minute will minimize any time response effects. Data for outdoor
391 and indoor sampling described in Sections 3.4 and 3.5 were therefore averaged to one minute.
392 During all experiments with gaseous reagents, no evidence of catalyst performance degradation
393 was observed.



394
 395 **Figure 4.** Allan-Werle deviation (3σ) in the HCl-TCl purged with zero-air (black line) shown
 396 with the ideal deviation (no drift, solid blue line) and associated error in the deviation (dashed
 397 blue line).

398 3.4. HCl-TCl applications to outdoor air

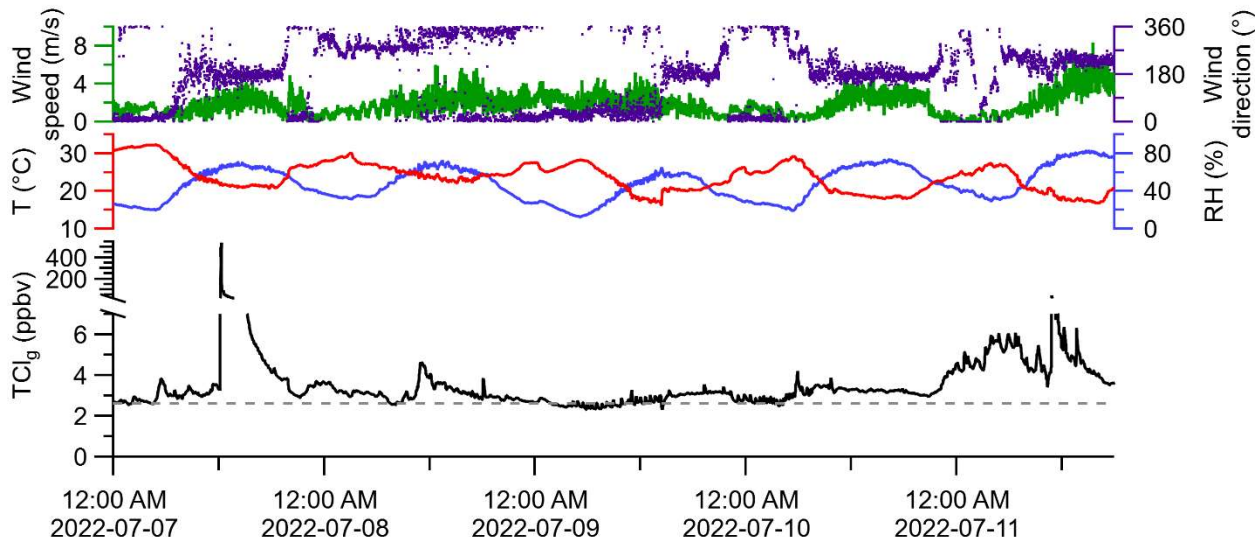
399 We deployed the system to measure ambient outdoor air, which we compare to the expected
 400 TCl_g range from complete thermolysis of previously measured Cl-containing compounds,
 401 estimated to be between 3.3 and 19 ppbv (Table S1). Global background levels of long-lived
 402 chlorine-containing species (LLCl_g) are well established (WMO (World Meteorological
 403 Organization), 2018) and were calculated by equation 3 using data from Table S1:

$$\begin{aligned}
 \text{404 } \text{LLCl}_g = & 3*[\text{CCl}_3\text{F}] + 2*[\text{CCl}_2\text{F}_2] + 4*[\text{CCl}_2\text{FCCl}_2\text{F}] + 4*[\text{CCl}_3\text{CClF}_2] + 3*[\text{CCl}_3\text{CF}_3] + \\
 \text{405 } & 2*[\text{CClF}_2\text{CClF}_2] + 2*[\text{CCl}_2\text{FCF}_3] + [\text{CClF}_2\text{CF}_3] + [\text{CHClF}_2] + [\text{CH}_2\text{ClCF}_3] + 2*[\text{CH}_3\text{CCl}_2\text{F}] + \\
 \text{406 } & [\text{CBrClF}_2] + 4*[\text{CCl}_4] \quad \text{E3}
 \end{aligned}$$

407 A global background for LLCl_g of approximately 2.6 ppbv is expected ((WMO (World
 408 Meteorological Organization), 2018), Table S1). The maximum, minimum, and median of
 409 observed ambient TCl_g were 536.3, 2.0, and 3.1 ppbv, respectively (Figure 5). Measurements of
 410 HCl alone were not made during these periods but reported ranges of HCl mixing ratios for this
 411 sampling location from Furlani et al. (2021) and Angelucci et al. (2021) were typically below 110
 412 pptv, with intermittent events up to 600 pptv. As expected, most ambient TCl_g measurements were

413 above the expected mixing ratio of LLCl_g . There is clear evidence of TCl_g sources beyond LLCl_g
414 at the sampling site, with several plumes of elevated TCl_g intercepted. For example, the maximum
415 TCl_g measurement (536.3 ppbv) was made in a plume just after noon on July 7. Another plume
416 was detected on July 11, with a maximum TCl_g of 42.1 ppbv. Though the purpose of this study
417 was not to determine sources of TCl_g , we observed that plumes containing elevated TCl_g arrived
418 from the S-SW of the sampling site, where several facilities that had reported tens to thousands of
419 kg of yearly emissions to air of Cl-containing species are located (Figure S5).

420



421

422 **Figure 5.** Monitoring meteorological conditions and one-minute averaged TCl_g in outdoor air
423 through HCl-TCl from July 7 to 11, 2022. Grey dashed line represents the background mixing
424 ratio for LLCl_g .

425 3.5. HCl-TCl application to indoor cleaning

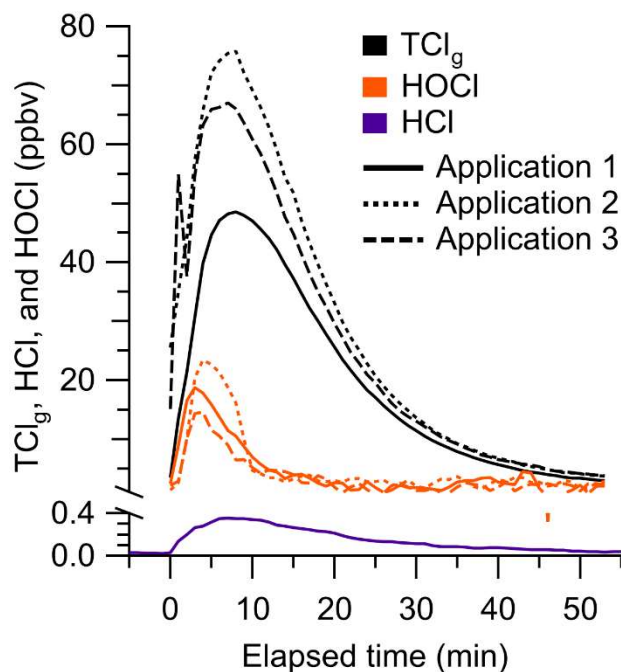
426 We applied a chlorine-based cleaning product four times in a well-lit indoor room and
427 measured TCl_g using the HCl-TCl and HOCl analyzer during three of the cleaning events (Figure
428 6). One cleaning experiment was done without the HCl-TCl and had a maximum of 370 pptv HCl.
429 These levels are comparable to peak HCl levels of ~ 500 pptv observed from surface application
430 of bleach (Dawe et al., 2019). Consistent with previous speciated measurements (Mattila et al.,

431 2020; Wong et al., 2017), HCl, HOCl, and TCl_g levels increased rapidly over ~5 minutes after the
432 application of the cleaning product. The maximum levels of TCl_g from HCl-TCl during application
433 1, 2, and 3, were 49.2, 80.0, and 69.7 ppbv, respectively. The maximum levels of HOCl from
434 applications 1, 2, and 3, were 19.6, 24.2, and 16.8 ppbv, respectively, corresponding to 24 to 40 %
435 of peak TCl_g and 14 to 22 % of integrated TCl_g. These TCl_g levels were several times higher than
436 most observed in outdoor air (Section 3.4) and were within the range expected from previous
437 experiments (Table S1). The levels of chlorinated species observed during bleaching events is
438 variable, between 15 to 100s of ppbv (Mattila et al., 2020; Odabasi, 2008; Wang et al., 2019; Wong
439 et al., 2017). By comparison, our highest observed mixing ratio was 80 ppbv. Because the
440 multiphase chemical processes involved in bleach application are complex and poorly understood,
441 it is difficult to compare levels between similar studies, given that the underlying ambient
442 conditions can be very different. In addition, physical parameters, such as volume of cleaning
443 solution applied, room size, and ventilation, can all affect observed mixing ratios. For example,
444 studies have observed that gaseous NH₃ partitioning into aqueous bleach can produce large and
445 variable amounts of chloramines, NH₂Cl, NHCl₂, and NCl₃ (Mattila et al., 2020; Wong et al.,
446 2017). In our experiments, there was on average 82 ± 4 % of integrated TCl_g that could not be
447 accounted for by the HOCl measurement. Additional chlorinated species that have previously been
448 observed to be emitted from surface bleaching include ClNO₂, NH₂Cl, NHCl₂, NCl₃, and several
449 chlorinated organics (Odabasi, 2008; Mattila et al., 2020; Wong et al., 2017) which likely also
450 contributed to our measured TCl_g. We observed that TCl_g decayed ~15% faster than the air
451 exchange rate (0.72 h⁻¹), indicating additional chemical loss pathways or surface interactions
452 (Figure S6). We observed a shorter lifetime of HOCl relative to TCl_g, which is consistent with
453 faster decay rates observed for HOCl and similar TCl_g species by Wong et. al., (2017). The HOCl

454 started decreasing after ~300 s had elapsed while the TCl_g levels were still increasing. This
455 suggests that reactions involving HOCl may have led to additional TCl_g species, which has been
456 observed in laboratory studies (Wang et al., 2019).

457 In-situ measurements of TCl_g could provide additional insight into sources of chlorinated
458 species to indoor environments by creating a total inventory from which the contributions of
459 individual measured species can be compared and used to elucidate unknown TCl_g levels and
460 mechanisms in real-time. Furthermore, several chlorinated species that have previously been
461 observed to be emitted from surface bleaching, including Cl₂, HOCl, ClNO₂, NH₂Cl, NHCl₂, and
462 NCl₃ (Mattila et al., 2020; Wong et al., 2017), have been measured by chemical ionization mass
463 spectrometry (CIMS). Quantifying chlorinated species using CIMS remains challenging due to the
464 required calibrations and difficulty in generating pure gas phase standards. It is therefore desirable
465 to have a technique such as the one proposed in this study that does not require calibrations or
466 knowledge of potential unknown TCl_g species. A combination of the two methods would help
467 constrain the total levels while still observing speciation for key TCl_g species.

468



469
 470 **Figure 6.** One-minute average HCl (purple), HOCl (orange), and TCl_g (black) observed during
 471 cleaning spray events. Mixing ratios were background corrected prior to each cleaning event. Each
 472 subsequent application of cleaner is illustrated by a lighter shade for HOCl and TCl_g.

473
 474 **4. Conclusions**

475 In this work we developed, optimized, validated, and applied a method capable of converting
 476 TCl_g into gaseous HCl for detection by CRDS. Our TCl_g measurement technique, the HCl-TCl, is
 477 composed of a platinum catalyst mesh inside a quartz glass flow tube all contained within a split-
 478 tube furnace. The temperature and flow rate were optimized at 825 °C and 1.5 seconds,
 479 respectively using DCM. These conditions were validated by the complete conversion of
 480 organochlorine compounds with strong C-Cl bonds. The HCl-TCl was used to measure TCl_g
 481 outdoors, observing a range of 2.0 to 536.3 ppbv. Levels mostly exceeded the expected background
 482 mixing ratio of LLCl_g. We also applied the HCl-TCl to an indoor environment during commercial
 483 bleach spray cleaning events and observed varying increases in TCl_g (50–80 ppbv), which was in
 484 reasonable agreement with levels observed in previous speciated measurements. The agreement of

485 HCl-TCl outdoor and indoor measurements with available bottom-up estimates indicates its
486 efficacy under real-world scenarios. Rapid changes in TCl_g were observed in both outdoor and
487 indoor environments indicating the utility of an in-situ technique to constrain the sources and
488 chemistry of TCl_g, as well as its impact on air quality, climate, and health. We anticipate this
489 approach could be used in several applications, including comparisons to speciated measurements
490 of chlorinated compounds and to further explore Cl reactivity and cycling with respect for indoor
491 and outdoor TCl_g.

492 **Acknowledgements**

493 We acknowledge the Sloan Foundation and Natural Sciences Engineering and Research Council
494 of Canada for funding. We thank Melodie Lao and Yashar Iranpour for collecting air exchange
495 rate data, Andrea Angelucci for collecting meteorological data, Dirk Verdoold for the custom
496 quartz tube, and Chris Caputo, John Liggio, Rob McLaren, and Trevor VandenBoer for helpful
497 discussions. PME thanks the European Research Council. TFK is a Canada Research Chair in
498 Environmental Analytical Chemistry. This work was undertaken, in part, thanks to funding from
499 the Canada Research Chairs program.

500 **Author contributions**

501 TCF, RY, JS, and LRC collected and analyzed the data. TCF, RY, LRC, and CJY conceived of
502 and designed the experiments with input from PME and TFK. Funding was obtained by TFK and
503 CJY. The manuscript was written by TCF, RY, and CJY with input from all authors.

504 **Data availability**

505 Outdoor and indoor datasets submitted to Federated Research Data Repository as Furlani, T.C.,
506 Ye, R., Stewart, J., Crilley, L.R., Edwards, P.M., Kahan, T.F., Young, C.J. (2022). Outdoor and

507 indoor gaseous total chlorine measurement in Toronto Canada. Federated Research Data
508 Repository. DOI will be updated when available.

509 **Competing interests**

510 The authors declare no competing interests.

511 **5. References**

- 512 Adcock, K. E., Reeves, C. E., Gooch, L. J., Leedham Elvidge, E. C., Ashfold, M. J.,
513 Brenninkmeijer, C. A. M., Chou, C., Fraser, P. J., Langenfelds, R. L., Mohd Hanif, N.,
514 O'Doherty, S., Oram, D. E., Ou-Yang, C.-F., Phang, S. M., Samah, A. A., Röckmann, T.,
515 Sturges, W. T., and Laube, J. C.: Continued increase of CFC-113a (CCl₃CF₃) mixing ratios in
516 the global atmosphere: emissions, occurrence and potential sources, *Atmos. Chem. Phys.*, 18,
517 4737–4751, <https://doi.org/10.5194/acp-18-4737-2018>, 2018.
- 518 Andrews, S. J., Carpenter, L. J., Apel, E. C., Atlas, E., Donets, V., Hopkins, J. R., Hornbrook, R.
519 S., Lewis, A. C., Lidster, R. T., Lueb, R., Minaeian, J., Navarro, M., Punjabi, S., Riemer, D., and
520 Schauffler, S.: A comparison of very short lived halocarbon (VSLS) and DMS aircraft
521 measurements in the tropical west Pacific from CAST, ATTREX and CONTRAST, *Atmos.*
522 *Meas. Tech.*, 9, 5213–5225, <https://doi.org/10.5194/amt-9-5213-2016>, 2016.
- 523 Berg, W. W., Crutzen, P. J., Grahek, F. E., Gitlin, S. N., and Sedlacek, W. A.: First
524 measurements of total chlorine and bromine in the lower stratosphere, *Geophys Res Lett*, 7, 937–
525 940, <https://doi.org/https://doi.org/10.1029/GL007i011p00937>, 1980.
- 526 Blankenship, A., Chang, D. P. Y., Jones, A. D., Kelly, P. B., Kennedy, I. M., Matsumura, F.,
527 Pasek, R., and Yang, G.: Toxic combustion by-products from the incineration of chlorinated
528 hydrocarbons and plastics, *Chemosphere*, 28, 183–196,
529 [https://doi.org/https://doi.org/10.1016/0045-6535\(94\)90212-7](https://doi.org/https://doi.org/10.1016/0045-6535(94)90212-7), 1994.
- 530 Butz, A., Dinger, A. S., Bobrowski, N., Kostinek, J., Fieber, L., Fischerkeller, C., Giuffrida, G.
531 B., Hase, F., Klappenbach, F., Kuhn, J., Lübcke, P., Tirpitz, L., and Tu, Q.: Remote sensing of
532 volcanic CO₂, HF, HCl, SO₂, and BrO in the downwind plume of Mt. Etna, *Atmos Meas Tech*,
533 10, 1–14, <https://doi.org/10.5194/amt-10-1-2017>, 2017.
- 534 Dawe, K. E. R., Furlani, T. C., Kowal, S. F., Kahan, T. F., Vandenboer, T. C., and Young, C. J.:
535 Formation and emission of hydrogen chloride in indoor air, *Indoor Air*, 70–78,
536 <https://doi.org/10.1111/ina.12509>, 2019.
- 537 Doucette, W. J., Wetzel, T. A., Dettenmaier, E., and Gorder, K.: Emission rates of chlorinated
538 volatile organics from new and used consumer products found during vapor intrusion
539 investigations: Impact on indoor air concentrations, *Environ Forensics*, 19, 185–190,
540 <https://doi.org/10.1080/15275922.2018.1475433>, 2018.

541 Fernando, S., Jobst, K. J., Taguchi, V. Y., Helm, P. A., Reiner, E. J., and McCarry, B. E.:
542 Identification of the Halogenated Compounds Resulting from the 1997 Plastimet Inc. Fire in
543 Hamilton, Ontario, using Comprehensive Two-Dimensional Gas Chromatography and
544 (Ultra)High Resolution Mass Spectrometry, *Environ Sci Technol*, 48, 10656–10663,
545 <https://doi.org/10.1021/es503428j>, 2014.

546 Finlayson-Pitts, B. J.: Chlorine Atoms as a Potential Tropospheric Oxidant in the Marine
547 Boundary Layer, *Research on Chemical Intermediates*, 19, 235–249,
548 <https://doi.org/10.1163/156856793X00091>, 1993.

549 Furlani, T. C., Veres, P. R., Dawe, K. E. R., Neuman, J. A., Brown, S. S., VandenBoer, T. C.,
550 and Young, C. J.: Validation of a new cavity ring-down spectrometer for measuring tropospheric
551 gaseous hydrogen chloride, *Atmos. Meas. Tech. Discuss.*, 2021, 1–30,
552 <https://doi.org/10.5194/amt-2021-105>, 2021.

553 Giardino, N. J. and Andelman, J. B.: Characterization of the emissions of trichloroethylene,
554 chloroform, and 1,2-dibromo-3-chloropropane in a full-size, experimental shower., *J Expo Anal*
555 *Environ Epidemiol*, 6, 413–423, 1996.

556 Hardy, J. E. and Knarr, J. J.: Technique for Measuring the Total Concentration of Gaseous Fixed
557 Nitrogen Species, *J Air Pollut Control Assoc*, 32, 376–379,
558 <https://doi.org/10.1080/00022470.1982.10465412>, 1982.

559 Haskins, J. D., Jaeglé, L., Shah, V., Lee, B. H., Lopez-Hilfiker, F. D., Campuzano-Jost, P.,
560 Schroder, J. C., Day, D. A., Guo, H., Sullivan, A. P., Weber, R., Dibb, J., Campos, T., Jimenez,
561 J. L., Brown, S. S., and Thornton, J. A.: Wintertime Gas-Particle Partitioning and Speciation of
562 Inorganic Chlorine in the Lower Troposphere Over the Northeast United States and Coastal
563 Ocean, *Journal of Geophysical Research: Atmospheres*, 123, 12,812-897,916,
564 <https://doi.org/10.1029/2018JD028786>, 2018.

565 Henschler, D.: Toxicity of Chlorinated Organic Compounds: Effects of the Introduction of
566 Chlorine in Organic Molecules, *Angewandte Chemie International Edition in English*, 33, 1920–
567 1935, <https://doi.org/https://doi.org/10.1002/anie.199419201>, 1994.

568 Kannan, K., Kawano, M., Kashima, Y., Matsui, M., and Giesy, J. P.: Extractable
569 Organohalogens (EOX) in Sediment and Biota Collected at an Estuarine Marsh near a Former
570 Chloralkali Facility, *Environ Sci Technol*, 33, 1004–1008, <https://doi.org/10.1021/es9811142>,
571 1999.

572 Kato, M., Urano, K., and Tasaki, T.: Development of Semi- and Nonvolatile Organic Halogen as
573 a New Hazardous Index of Flue Gas, *Environ Sci Technol*, 34, 4071–4075,
574 <https://doi.org/10.1021/es000881+>, 2000.

575 Kawano, M., Falandysz, J., and Wakimoto, T.: Instrumental neutron activation analysis of
576 extractable organohalogens in the Antarctic Weddell seal (*Leptonychotes weddelli*), *J*
577 *Radioanal Nucl Chem*, 272, 501–504, <https://doi.org/10.1007/s10967-007-0611-5>, 2007.

578 Keene, William. C., Khalil, M. A. K., Erickson, David. J., McCulloch, A., Graedel, T. E., Lobert,
579 J. M., Aucott, M. L., Gong, S. L., Harper, D. B., Kleiman, G., Midgley, P., Moore, R. M.,
580 Seuzaret, C., Sturges, W. T., Benkovitz, C. M., Koropalov, V., Barrie, L. A., and Li, Y. F.:
581 Composite global emissions of reactive chlorine from anthropogenic and natural sources:
582 Reactive Chlorine Emissions Inventory, *Journal of Geophysical Research: Atmospheres*, 104,
583 8429–8440, <https://doi.org/10.1029/1998JD100084>, 1999.

584 Khalil, M. A. K., Moore, R. M., Harper, D. B., Lobert, J. M., Erickson, D. J., Koropalov, V.,
585 Sturges, W. T., and Keene, W. C.: Natural emissions of chlorine-containing gases: Reactive
586 Chlorine Emissions Inventory, *Journal of Geophysical Research: Atmospheres*, 104, 8333–8346,
587 <https://doi.org/10.1029/1998JD100079>, 1999.

588 Lao, M., Crilley, L. R., Salehpoor, L., Furlani, T. C., Bourgeois, I., Neuman, J. A., Rollins, A.
589 W., Veres, P. R., Washenfelder, R. A., Womack, C. C., Young, C. J., and VandenBoer, T. C.: A
590 portable, robust, stable and tunable calibration source for gas-phase nitrous acid (HONO), *Atmos*
591 *Meas Tech*, 13, 5873–5890, <https://doi.org/10.5194/amt-13-5873-2020>, 2020.

592 Lobert, J. M., Keene, W. C., Logan, J. A., and Yevich, R.: Global chlorine emissions from
593 biomass burning: Reactive Chlorine Emissions Inventory, *Journal of Geophysical Research*
594 *Atmospheres*, 104, 8373–8389, <https://doi.org/10.1029/1998JD100077>, 1999.

595 Maris, C., Chung, M. Y., Lueb, R., Krischke, U., Meller, R., Fox, M. J., and Paulson, S. E.:
596 Development of instrumentation for simultaneous analysis of total non-methane organic carbon
597 and volatile organic compounds in ambient air, *Atmos Environ*, 37, 149–158,
598 [https://doi.org/https://doi.org/10.1016/S1352-2310\(03\)00387-X](https://doi.org/https://doi.org/10.1016/S1352-2310(03)00387-X), 2003.

599 Massin, N., Bohadana, A. B., Wild, P., Héry, M., Toamain, J. P., and Hubert, G.: Respiratory
600 symptoms and bronchial responsiveness in lifeguards exposed to nitrogen trichloride in indoor
601 swimming pools., *Occup Environ Med*, 55, 258 LP – 263, <https://doi.org/10.1136/oem.55.4.258>,
602 1998.

603 Mattila, J. M., Lakey, P. S. J., Shiraiwa, M., Wang, C., Abbatt, J. P. D., Arata, C., Goldstein, A.
604 H., Ampollini, L., Katz, E. F., DeCarlo, P. F., Zhou, S., Kahan, T. F., Cardoso-Saldaña, F. J.,
605 Ruiz, L. H., Abeleira, A., Boedicker, E. K., Vance, M. E., and Farmer, D. K.: Multiphase
606 Chemistry Controls Inorganic Chlorinated and Nitrogenated Compounds in Indoor Air during
607 Bleach Cleaning, *Environ Sci Technol*, 54, 1730–1739, <https://doi.org/10.1021/acs.est.9b05767>,
608 2020.

609 Miyake, Y., Kato, M., and Urano, K.: A method for measuring semi- and non-volatile organic
610 halogens by combustion ion chromatography, *J Chromatogr A*, 1139, 63–69,
611 <https://doi.org/https://doi.org/10.1016/j.chroma.2006.10.078>, 2007a.

612 Miyake, Y., Yamashita, N., Rostkowski, P., So, M. K., Taniyasu, S., Lam, P. K. S., and Kannan,
613 K.: Determination of trace levels of total fluorine in water using combustion ion chromatography
614 for fluorine: A mass balance approach to determine individual perfluorinated chemicals in water,
615 *J Chromatogr A*, 1143, 98–104, <https://doi.org/https://doi.org/10.1016/j.chroma.2006.12.071>,
616 2007b.

617 Miyake, Y., Yamashita, N., So, M. K., Rostkowski, P., Taniyasu, S., Lam, P. K. S., and Kannan,
618 K.: Trace analysis of total fluorine in human blood using combustion ion chromatography for
619 fluorine: A mass balance approach for the determination of known and unknown organofluorine
620 compounds, *J Chromatogr A*, 1154, 214–221,
621 <https://doi.org/https://doi.org/10.1016/j.chroma.2007.03.084>, 2007c.

622 Montzka, S. A., Dutton, G. S., Portmann, R. W., Chipperfield, M. P., Davis, S., Feng, W.,
623 Manning, A. J., Ray, E., Rigby, M., Hall, B. D., Siso, C., Nance, J. D., Krummel, P. B., Mühle,
624 J., Young, D., O’Doherty, S., Salameh, P. K., Harth, C. M., Prinn, R. G., Weiss, R. F., Elkins, J.
625 W., Walter-Terrinoni, H., and Theodoridi, C.: A decline in global CFC-11 emissions during
626 2018–2019, *Nature*, 590, 428–432, <https://doi.org/10.1038/s41586-021-03260-5>, 2021.

627 Nuckols, J. R., Ashley, D. L., Lyu, C., Gordon, S. M., Hinckley, A. F., and Singer, P.: Influence
628 of tap water quality and household water use activities on indoor air and internal dose levels of
629 trihalomethanes, *Environ Health Perspect*, 113, 863–870, <https://doi.org/10.1289/ehp.7141>,
630 2005.

631 Odabasi, M.: Halogenated Volatile Organic Compounds from the Use of Chlorine-Bleach-
632 Containing Household Products, *Environ Sci Technol*, 42, 1445–1451,
633 <https://doi.org/10.1021/es702355u>, 2008.

634 Odabasi, M., Elbir, T., Dumanoglu, Y., and Sofuoglu, S.: Halogenated volatile organic
635 compounds in chlorine-bleach-containing household products and implications for their use,
636 *Atmos Environ*, 92, 376–383, <https://doi.org/10.1016/j.atmosenv.2014.04.049>, 2014.

637 Pan, L. L., Atlas, E. L., Salawitch, R. J., Honomichl, S. B., Bresch, J. F., Randel, W. J., Apel, E.
638 C., Hornbrook, R. S., Weinheimer, A. J., Anderson, D. C., Andrews, S. J., Baidar, S., Beaton, S.
639 P., Campos, T. L., Carpenter, L. J., Chen, D., Dix, B., Donets, V., Hall, S. R., Hanisco, T. F.,
640 Homeyer, C. R., Huey, L. G., Jensen, J. B., Kaser, L., Kinnison, D. E., Koenig, T. K., Lamarque,
641 J.-F., Liu, C., Luo, J., Luo, Z. J., Montzka, D. D., Nicely, J. M., Pierce, R. B., Riemer, D. D.,
642 Robinson, T., Romashkin, P., Saiz-Lopez, A., Schauffler, S., Shieh, O., Stell, M. H., Ullmann,
643 K., Vaughan, G., Volkamer, R., and Wolfe, G.: The Convective Transport of Active Species in
644 the Tropics (CONTRAST) Experiment, *Bull Am Meteorol Soc*, 98, 106–128,
645 <https://doi.org/10.1175/BAMS-D-14-00272.1>, 2017.

646 Prinn, R. G., Weiss, R. F., Arduini, J., Arnold, T., DeWitt, H. L., Fraser, P. J., Ganesan, A. L.,
647 Gasore, J., Harth, C. M., Hermansen, O., Kim, J., Krummel, P. B., Li, S., Loh, Z. M., Lunder, C.
648 R., Maione, M., Manning, A. J., Miller, B. R., Mitrevski, B., Mühle, J., O’Doherty, S., Park, S.,
649 Reimann, S., Rigby, M., Saito, T., Salameh, P. K., Schmidt, R., Simmonds, P. G., Steele, L. P.,
650 Vollmer, M. K., Wang, R. H., Yao, B., Yokouchi, Y., Young, D., and Zhou, L.: History of
651 chemically and radiatively important atmospheric gases from the Advanced Global Atmospheric
652 Gases Experiment (AGAGE), *Earth Syst. Sci. Data*, 10, 985–1018, <https://doi.org/10.5194/essd-10-985-2018>, 2018.

654 Raff, J. D., Njegic, B., Chang, W. L., Gordon, M. S., Dabdub, D., Gerber, R. B., and Finlayson-
655 Pitts, B. J.: Chlorine activation indoors and outdoors via surface-mediated reactions of nitrogen

656 oxides with hydrogen chloride, *Proceedings of the National Academy of Sciences*, 106, 13647
657 LP – 13654, <https://doi.org/10.1073/pnas.0904195106>, 2009.

658 Riedel, T. P., Wolfe, G. M., Danas, K. T., Gilman, J. B., Kuster, W. C., Bon, D. M., Vlasenko,
659 A., Li, S.-M., Williams, E. J., Lerner, B. M., Veres, P. R., Roberts, J. M., Holloway, J. S., Lefer,
660 B., Brown, S. S., and Thornton, J. A.: An MCM modeling study of nitryl chloride (ClNO₂)
661 impacts on oxidation, ozone production and nitrogen oxide partitioning in polluted continental
662 outflow, *Atmos. Chem. Phys.*, 14, 3789–3800, <https://doi.org/10.5194/acp-14-3789-2014>, 2014.

663 Roberts, J. M., Bertman, S. B., Jobson, T., Niki, H., and Tanner, R.: Measurement of total
664 nonmethane organic carbon (C_y): Development and application at Chebogue Point, Nova Scotia,
665 during the 1993 North Atlantic Regional Experiment campaign, *Journal of Geophysical*
666 *Research: Atmospheres*, 103, 13581–13592, <https://doi.org/10.1029/97JD02240>,
667 1998.

668 Saiz-Lopez, A. and Von Glasow, R.: Reactive halogen chemistry in the troposphere, *Chem Soc*
669 *Rev*, 41, 6448–6472, <https://doi.org/10.1039/c2cs35208g>, 2012.

670 Schwartz-Narbonne, H., Wang, C., Zhou, S., Abbatt, J. P. D., and Faust, J.: Heterogeneous
671 Chlorination of Squalene and Oleic Acid, *Environ Sci Technol*, 53, 1217–1224,
672 <https://doi.org/10.1021/acs.est.8b04248>, 2019.

673 Shepherd, J. L., Corsi, R. L., and Kemp, J.: Chloroform in Indoor Air and Wastewater: The Role
674 of Residential Washing Machines., *J Air Waste Manag Assoc*, 46, 631–642,
675 <https://doi.org/10.1080/10473289.1996.10467497>, 1996.

676 Sherwen, T., Schmidt, J. A., Evans, M. J., Carpenter, L. J., Großmann, K., Eastham, S. D., Jacob,
677 D. J., Dix, B., Koenig, T. K., Sinreich, R., Ortega, I., Volkamer, R., Saiz-Lopez, A., Prados-
678 Roman, C., Mahajan, A. S., and Ordóñez, C.: Global impacts of tropospheric halogens (Cl, Br, I)
679 on oxidants and composition in GEOS-Chem, *Atmos. Chem. Phys.*, 16, 12239–12271,
680 <https://doi.org/10.5194/acp-16-12239-2016>, 2016.

681 Simpson, W. R., Brown, S. S., Saiz-Lopez, A., Thornton, J. A., and Von Glasow, R.:
682 Tropospheric Halogen Chemistry: Sources, Cycling, and Impacts, *Chem Rev*, 115, 4035–4062,
683 <https://doi.org/10.1021/cr5006638>, 2015.

684 Solomon, S.: Stratospheric ozone depletion: A review of concepts and history, *Reviews of*
685 *Geophysics*, 37, 275–316, <https://doi.org/10.1029/1999RG900008>, 1999.

686 Stockwell, C. E., Kupc, A., Witkowski, B., Talukdar, R. K., Liu, Y., Selimovic, V., Zarzana, K.
687 J., Sekimoto, K., Warneke, C., Washenfelder, R. A., Yokelson, R. J., Middlebrook, A. M., and
688 Roberts, J. M.: Characterization of a catalyst-based conversion technique to measure total
689 particulate nitrogen and organic carbon and comparison to a particle mass measurement
690 instrument, *Atmos. Meas. Tech.*, 11, 2749–2768, <https://doi.org/10.5194/amt-11-2749-2018>,
691 2018.

692 Stubbs, A., Lao, M., Wang, C., Abbatt, J., Hoffnagle, J., VandenBoer, T., and Kahan, T.: Near-
693 source hypochlorous acid emissions from indoor bleach cleaning, *Environ Sci Process Impacts*,
694 Submitted, 2022.

695 Unsal, V., Cicek, M., and Sabancilar, İ.: Toxicity of carbon tetrachloride, free radicals and role
696 of antioxidants, *Rev Environ Health*, 36, 279–295, <https://doi.org/doi:10.1515/reveh-2020-0048>,
697 2021.

698 Veres, P., Gilman, J. B., Roberts, J. M., Kuster, W. C., Warneke, C., Burling, I. R., and de
699 Gouw, J.: Development and validation of a portable gas phase standard generation and
700 calibration system for volatile organic compounds, *Atmos. Meas. Tech.*, 3, 683–691,
701 <https://doi.org/10.5194/amt-3-683-2010>, 2010.

702 Wang, C., Collins, D. B., and Abbatt, J. P. D.: Indoor Illumination of Terpenes and Bleach
703 Emissions Leads to Particle Formation and Growth, *Environ Sci Technol*, 53, 11792–11800,
704 <https://doi.org/10.1021/acs.est.9b04261>, 2019.

705 White, C. W. and Martin, J. G.: Chlorine Gas Inhalation, *Proc Am Thorac Soc*, 7, 257–263,
706 <https://doi.org/10.1513/pats.201001-008SM>, 2010.

707 WMO (World Meteorological Organization): Scientific Assessment of Ozone Depletion: 2018,
708 Report No., Global Ozone Research and Monitoring Project, Geneva, Switzerland, 588 pp. pp.,
709 2018.

710 Wong, J. P. S., Carslaw, N., Zhao, R., Zhou, S., and Abbatt, J. P. D.: Observations and impacts
711 of bleach washing on indoor chlorine chemistry, *Indoor Air*, 27, 1082–1090,
712 <https://doi.org/10.1111/ina.12402>, 2017.

713 Xu, D., Zhong, W., Deng, L., Chai, Z., and Mao, X.: Levels of Extractable Organohalogenes in
714 Pine Needles in China, *Environ Sci Technol*, 37, 1–6, <https://doi.org/10.1021/es025799o>, 2003.

715 Xu, D., Tian, Q., and Chai, Z.: Determination of extractable organohalogenes in the atmosphere
716 by instrumental neutron activation analysis, *J Radioanal Nucl Chem*, 270, 5–8,
717 <https://doi.org/10.1007/s10967-006-0302-7>, 2006.

718 Xu, D., Dan, M., Song, Y., Chai, Z., and Zhuang, G.: Instrumental neutron activation analysis of
719 extractable organohalogenes in PM_{2.5} and PM₁₀ in Beijing, China, *J Radioanal Nucl Chem*, 271,
720 115–118, <https://doi.org/10.1007/s10967-007-0115-3>, 2007.

721 Yang, M. and Fleming, Z. L.: Estimation of atmospheric total organic carbon (TOC) – paving the
722 path towards carbon budget closure, *Atmos Chem Phys*, 19, 459–471,
723 <https://doi.org/10.5194/acp-19-459-2019>, 2019.

724 Yeung, L. W. Y., Miyake, Y., Taniyasu, S., Wang, Y., Yu, H., So, M. K., Jiang, G., Wu, Y., Li,
725 J., Giesy, J. P., Yamashita, N., and Lam, P. K. S.: Perfluorinated Compounds and Total and
726 Extractable Organic Fluorine in Human Blood Samples from China, *Environ Sci Technol*, 42,
727 8140–8145, <https://doi.org/10.1021/es800631n>, 2008.

728 Young, C. J., Washenfelder, R. A., Edwards, P. M., Parrish, D. D., Gilman, J. B., Kuster, W. C.,
729 Mielke, L. H., Osthoff, H. D., Tsai, C., Pikel'naya, O., Stutz, J., Veres, P. R., Roberts, J. M.,
730 Griffith, S., Dusanter, S., Stevens, P. S., Flynn, J., Grossberg, N., Lefer, B., Holloway, J. S.,
731 Peischl, J., Ryerson, T. B., Atlas, E. L., Blake, D. R., and Brown, S. S.: Chlorine as a primary
732 radical: Evaluation of methods to understand its role in initiation of oxidative cycles, *Atmos*
733 *Chem Phys*, 14, 3427–3440, <https://doi.org/10.5194/acp-14-3427-2014>, 2014.

734 Zhai, S., Wang, X., McConnell, J. R., Geng, L., Cole-Dai, J., Sigl, M., Chellman, N., Sherwen,
735 T., Pound, R., Fujita, K., Hattori, S., Moch, J. M., Zhu, L., Evans, M., Legrand, M., Liu, P.,
736 Pasteris, D., Chan, Y.-C., Murray, L. T., and Alexander, B.: Anthropogenic Impacts on
737 Tropospheric Reactive Chlorine Since the Preindustrial, *Geophys Res Lett*, 48, e2021GL093808,
738 <https://doi.org/https://doi.org/10.1029/2021GL093808>, 2021.

739 Zhang, W., Jiao, Y., Zhu, R., Rhew, R. C., Sun, B., and Dai, H.: Chloroform (CHCl₃) Emissions
740 From Coastal Antarctic Tundra, *Geophys Res Lett*, 48, e2021GL093811,
741 <https://doi.org/https://doi.org/10.1029/2021GL093811>, 2021.

742